RESEARCH ARTICLE

Exploiting Phase Difference of Arrival of V2X Signals for Pedestrian Positioning: Key Methods and Simulation Evaluation

SUHUA TANG [ID]1, **(Senior Member, IEEE), AND SADAO OBANA**2

1Department of Computer and Network Engineering, The University of Electro-Communications, Chofu, Tokyo 182-8585, Japan
2The University of Electro-Communications, Chofu, Tokyo 182-8585, Japan

Corresponding author: Suhua Tang (shtang@uec.ac.jp)

ABSTRACT Pedestrian-to-vehicle communication helps to prevent pedestrian accidents by disseminating position information of a pedestrian to nearby vehicles. This is especially useful when a pedestrian is in the blind spot of vehicles. In urban canyons, roadside buildings obstruct satellite signals, which may cause an outage in pedestrian positioning. Using vehicles and roadside units as positioning anchors helps to solve this problem. But the performance of distance estimation, based on the attenuation property of wireless signals, is degraded by multipath propagation. To address this issue, this paper exploits phase information of V2X signals, instead of signal strength, for distance estimation. The signal transmitted by a pedestrian device is simultaneously received by several anchors, and the phase difference of arrival (PDoA) is used to compute the distance difference. Using the OFDM structure, phase information of multiple subcarriers can be computed efficiently. Potential problems like inter-symbol interference, synchronization error and phase ambiguity are addressed and the accuracy of distance estimation is further improved by combining phase information of multiple subcarriers before fixing the phase ambiguity. The effectiveness of the proposed method is verified by simulation evaluations, using 3D map and ray-tracing.

INDEX TERMS Pedestrian positioning, V2X, vehicle-to-everything, OFDM, PDoA, phase difference of arrival.

I. INTRODUCTION

Vehicles have greatly changed our life ever since their invention, with both pros and cons. On the one hand, our mobility becomes very convenient. On the other hand, many traffic accidents occur every year, not to mention the cost of traffic congestion in the rush hours. According to the yearly report on traffic safety by Cabinet Office of Japan, traffic fatalities are divided into five types, and the percentage of pedestrian fatalities is the highest, nearly one third in Japan [1]. In this sense, pedestrians are vulnerable road users, and may be seriously injured or even die once involved in an accident.

The associate editor coordinating the review of this manuscript and approving it for publication was Chao Zuo [ID].

These days, many vehicles use some onboard sensors, e.g., camera, Radar and LiDAR, to help detect nearby pedestrians in case the driver misses them. But these sensors do not work well when pedestrians happen to stay in the blind spot of vehicles. In such cases, pedestrian-to-vehicle communication [2], disseminating pedestrian position to nearby vehicles, helps vehicles to better sense the presence of pedestrians, and the performance can be further improved by the prediction of pedestrian behaviour [3].

GNSS (Global Navigation Satellite System) is the typical method for pedestrian positioning, and there is a trend of integrating multiple satellite systems, e.g., GPS, Galileo, Beidou, so as to increase the number of satellites. Phase information of satellite signals, usually exploited to realize RTK(Real Time Kinematic)-GNSS in high-end positioning devices, now is also explored for more accurate positioning

in mobile devices such as smartphones [4]. But in urban canyons, due to the obstruction of roadside buildings, most directly visible satellites are located overhead and seriously biased, where a small error in distance estimation may lead to a large error in position.

Fortunately, the new V2X (vehicle-to-everything) communication techniques have paved a new way for pedestrian positioning, where vehicles and roadside units (RSUs) can be used as positioning anchors [5], [6]. Both IEEE 802.11bd as a successor of 802.11p [7] and Cellular V2X [8] defined as a part of 5G (The Fifth Generation of Mobile Telephony) specification by 3GPP (3rd Generation Partnership Project) will support the communication between vehicles and pedestrians. Compared with pedestrian devices, a vehicle will achieve much higher positioning accuracy, by integrating onboard sensors with high-accuracy RTK-GNSS positioning [9]. Meanwhile, it is expected that many RSUs will be installed to provide network access to vehicles, which can be used as positioning anchors as well. In addition, vehicles and RSUs are located at the same height as pedestrians, and placed in a more balanced way, compared with satellites. Therefore, they can be good anchors for pedestrian positioning.

Generally, pedestrian positioning can be performed in two modes. In the user-based mode, a pedestrian device computes the position by itself, and needs to receive signals from anchors continuously, which leads to much power consumption. The other is network-based mode, in which a pedestrian device transmits packets periodically and nearby anchors receive the signal and help compute pedestrian position. Interested readers may refer to the review paper [10] for more details on network-based positioning in the 5G and 6G networks.

In outdoor scenarios, because the environment keeps changing, pedestrian positioning usually exploits the trilateration method, and wireless signal is used to estimate pedestrian-anchor distances. Previous work has exploited signal strength-based (simple but with low accuracy) [5], [11], [12], time-based (high accuracy but susceptible to synchronization error) [13], [14], and phased based methods (high accuracy but with low efficiency) [15], [16], [17] for distance estimation. But it is difficult to achieve high accuracy and efficiency at the same time.

In this work, we study network-based positioning, and leverage phase information of V2X signals, instead of signal strength, for distance estimation. The main advantage of using phase information is that it is less susceptible to multipath and noise compared with signal strength. The signal transmitted by a pedestrian device is simultaneously received by several anchors (e.g., RSUs), and the phase difference of arrival (PDoA) is used to compute the distance difference. Using the OFDM (Orthogonal Frequency-Division Multiplexing) structure, phase information of multiple subcarriers is computed efficiently, simultaneously at multiple anchors. Potential problems like inter-symbol interference (ISI), synchronization error and phase ambiguity are addressed and the accuracy of distance estimation is improved by combining

phase information of multiple subcarriers before fixing the phase ambiguity. Simulation evaluations, based on 3D map and ray-tracing, confirm the effectiveness of the proposed method.

The contribution of this paper is four-fold, as follows.

- Dealing with ISI. Computing PDoA requires to sample OFDM signals simultaneously at different anchors, which may lead to the ISI problem. A simple method is proposed to adjust the sampling time at different anchors, which does not affect the estimation of distance difference.
- Dealing with synchronization error. Synchronization error, which often occurs in real systems, is converted to the less severe ISI error. In this way, PDoA is less susceptible to synchronization error compared with the TDoA (Time Difference of Arrival) method.
- Dealing with multipath and noise. Frequency pairs are divided into groups, each group having the same frequency difference. We fuse distance differences computed from different groups, which helps to resist multipath and noise.
- Solving phase ambiguity. In each group of frequency pairs, we fuse the distance difference, which helps to reduce the noise and fix the phase ambiguity.

Part of this work, mainly the first point, has been reported in a conference paper [18]. In this paper, the second and the fourth points are newly added and the third point is enhanced. In the evaluation, 3D map and ray-tracing are used to emulate multipath propagation. The communication process of OFDM signals is simulated. From the attenuated and noisy signal, time synchronization is performed, phase is computed, and distance difference is estimated. Evaluation results confirm the effectiveness of the proposed method in suppressing noise and multipath waves, and its superiority over TDoA in multipath-rich urban environments.

The rest of this paper is organized as follows: Sec. II reviews related work. Sec. III presents the system model and points out error factors. Then, Sec. IV proposes methods to deal with these error factors respectively. Sec. V shows the evaluation setting and results in the multipath-rich environment. Finally, Sec. VI concludes this paper.

II. RELATED WORK

In the outdoor environment, the trilateration method usually is used to compute pedestrian position. It relies on the estimation of pedestrian-anchor distances. Previous work in this field can be classified into 3 categories, as follows:

(i) Signal-strength-based methods. It is well known that path loss in the wireless environment increases with the distance, which is often used to predict the propagation distance. Path loss is computed from the difference between transmission power and RSSI (Received Signal Strength Indicator). Because RSSI is greatly affected by multipath propagation, the corresponding distance error is large.

When transmitting a signal in a wideband system, the direct wave and its reflected replicas arrive at a receiver at different

timing. As a result, it is possible to get the signal strength of the direct wave from CSI (channel state information) and use it to predict the distance [5], [11], [12], which is more accurate than using RSSI. But when the time resolution is not high enough, a reflected wave may overlap the direct one, which degrades the performance.

(ii) Time-based methods. Because the propagation speed of a wireless signal is almost constant in the air, it is possible to compute the distance from the time-of-flight (ToF). When a transmitter and a receiver is synchronized in time, ToF is the difference between the time-of-arrival (ToA) at the receiver and the time-of-departure (ToD) at the transmitter. In order to relax the synchronization requirement, IEEE 802.11mc has defined FTM (fine time measurement), a procedure for estimating ToF between the transmitter and receiver by exchanging a sequence of messages with ToA and ToD. But this not only causes much overhead but also leads to a large delay in position computation [19]. The measurements of ToA and ToD depend on specific RF chains. As a result, FTM tends to have a poor accuracy [20], and it requires a calibration for each pair of transmitter and receiver to achieve a high accuracy [21]. In an ultra-wideband system, the ToF can be measured more accurately by using a larger bandwidth, and its combination with inertial measurement unit is studied in [14], which helps mitigate the outage probability.

Strict synchronization between a transmitter and a receiver is non-trivial. An alternative method is to compute the TDoA as the difference of ToAs at two receivers synchronized in time [22]. In [13], an IEEE 802.11g signal from a transmitter is received simultaneously by two synchronized receivers, and ToA is estimated based on the long training symbols. Then, TDoA is used to compute the distance difference to two receivers. But it is susceptible to the synchronization error.

(iii) Phase-based methods. It is known that the phase of a wireless signal changes with the propagation distance, linearly if the phase is not wrapped to the range of $[0, 2\pi)$. This property is exploited for the distance estimation in the RFID field [15], [16]. Usually, PDoA achieves higher accuracy than TDoA in distance estimation [17]. But the phase wrapping does occur, which leads to phase ambiguity: the number of 2π periods is unknown and needs to be fixed before using the phase to compute the distance. Many works assume that PDoA is already measured and focus on the position computation, using PDoA alone, or jointly exploiting TDoA and PDoA [17]. In the few works that discuss phase measurement [15], [16], usually the phase of each frequency is estimated successively, which is time consuming.

In this paper, aiming to improve system efficiency, we leverage OFDM signals to simultaneously measure the phases of multiple frequencies, and discuss potential problems and solutions.

III. SYSTEM MODEL
It is assumed that a pedestrian device periodically broadcasts a V2X OFDM signal, announcing its presence to nearby
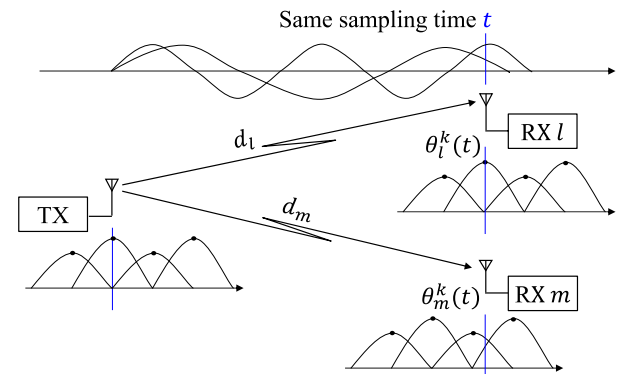

FIGURE 1. System model for measuring distance difference from a transmitter (pedestrian) to two receivers (anchors) based on phase difference of arrival.

vehicles. This signal is received by several nearby anchors (RSUs or vehicles). These anchors are synchronized in time and connected to a common server, where the distance difference is estimated. Figure 1 shows an example with two receivers. The distances from the transmitter to a receiver $r = l, m$ is d_r. The OFDM signal contains N orthogonal frequencies with an equal space Δf. N samples, with an interval $T_s = 1/(N \cdot \Delta f)$ in time, are acquired per receiver, starting from the same time t. The phases of arrival of N frequencies at receiver r and time t, $\theta_r^k(t)$, $k = 0, 1, \cdots, N - 1$, are computed by fast Fourier transform. Then, the distance difference, $d_l - d_m$, is computed from the phase information.

A. PHASE COMPUTATION BY OFDM
In the V2X OFDM signal, N subcarriers (frequencies), orthogonal to each other, are used at the same time. Adjacent subcarriers have the same frequency interval Δf, and in the time domain the sampling timing, with an interval T_s, is set as follows:

$$f_k - f_0 = k \cdot \Delta f, k = 0, 1, \cdots, N - 1,$$
$$t = nT_s, T_s = 1/(N \cdot \Delta f), n = 0, 1, \cdots, N - 1. \quad (1)$$

$f(t)$, as a pulse shaping signal, is used to ensure that the spectrum of the OFDM signal will not leak outside the allocated bandwidth. Usually $f(t) \neq 0$ at $t \neq nT_s$ and $f(t) = 0$ at $t = nT_s, n \neq 0$. Therefore, a sampling time offset will lead to the ISI problem.

Consider the processing of the k-th subcarrier at receiver r. Its phase at time t is $\theta_r^k(t)$. Then, N consecutive samples from time t, obtained at an equal interval T_s, are

$$x_n = \sum_i \alpha_{r,k} \exp(j(2\pi \frac{k \cdot i}{N} + \theta_r^k(t)))f(t + nT_s - iT_s),$$
$$n = 0, 1, \cdots, N - 1, \quad (2)$$

where $\alpha_{r,k}$ represents the amplitude of the k-th subcarrier, while $\theta_r^k(t)$ includes the phase information caused by modulation data and channel propagation. $f(\cdot)$ disappears when the sampling time is synchronized, and $x_n = \alpha_{r,k} \exp(j(2\pi \frac{k \cdot n}{N} + \theta_r^k(t)))$ by assuming $t = 0$. By applying fast Fourier
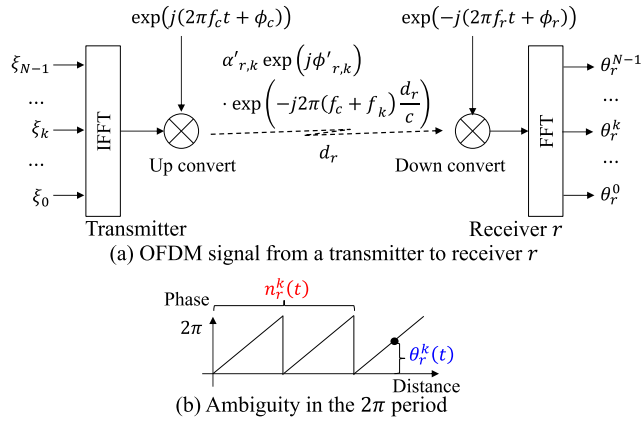
FIGURE 2. Phase variation of an OFDM signal with respect to the propagation distance. Phase wrapping leads to the ambiguity in the 2π periods.

transform (FFT) to the N samples, the coefficient of the k-th subcarrier is

$$F_r^k = N\alpha_{r,k} \exp(j\theta_r^k(t)), \tag{3}$$

from which $\theta_r^k(t)$ is computed as

$$\theta_r^k(t) = \angle F_r^k. \tag{4}$$

B. RELATION BETWEEN DISTANCE AND PHASE
Because the subcarriers are orthogonal, in the following we focus on a single subcarrier $f_k, k = 0, 1, \ldots, N-1$ and a receiver $r, r = l, m$ in Figure 2(a). At the transmitter, subcarrier f_k, modulated by user data $\xi_k = \alpha_k' \exp(j\phi_k')$, is

$$\alpha_k' \exp(j\phi_k') \cdot \exp(j2\pi f_k t). \tag{5}$$

Using a carrier signal $\exp(j(2\pi f_c t + \phi_c))$, this signal is shifted to the RF band, as follows:

$$s_k(t) = \alpha_k' \cdot \exp(j(2\pi(f_c + f_k)t + \phi_k' + \phi_c)). \tag{6}$$

The complex channel gain, between the transmitter and receiver r ($r = l, m$) with a distance d_r away, is $\alpha_{r,k}' \exp(j\phi_{r,k}') \cdot \exp(-j2\pi(f_c + f_k)d_r/c)$. $\alpha_{r,k}'$ represents the channel attenuation, which varies with the distance and is greatly affected by multipath fading. $\phi_{r,k}'$ is an extra phase variation caused by potential reflection or diffraction, and is 0 for a line-of-sight (LoS) wave. The phase variation related to propagation distance d_r and light speed c will be leveraged for the distance estimation.

At receiver r, the signal is shifted back to the baseband, using a carrier signal $\exp(-j(2\pi f_r t + \phi_r))$. And the phase of the LoS part corresponding to subcarrier f_k is

$$(f_c + f_k - f_r)t - (f_c + f_k)\frac{d_r}{c} + \frac{1}{2\pi}(\phi_k' + \phi_c - \phi_r)$$
$$= n_r^k(t) + \frac{1}{2\pi}\theta_r^k(t), r = l, m. \tag{7}$$

It consists of two parts. $\theta_r^k(t) \in [0, 2\pi)$ is the directly measured phase (wrapped phase) while $n_r^k(t)$ is an integer

denoting the phase ambiguity of 2π periods, as shown in Figure 2(b). $n_r^k(t)$ needs to be fixed before computing d_r.

To remove the impact of carrier frequency, we consider the phase difference of two subcarriers f_p and f_q at receiver r. By replacing k with p and q in (7), and taking the subtraction, the phase difference, $\theta_r^{p,q}(t) = \theta_r^p(t) - \theta_r^q(t)$, is computed as

$$(f_p - f_q)t - (f_p - f_q)\frac{d_r}{c} + \frac{1}{2\pi}(\phi_p' - \phi_q')$$
$$= n_r^{p,q}(t) + \frac{1}{2\pi}\theta_r^{p,q}(t), \tag{8}$$

where $n_r^{p,q}(t) = n_r^p(t) - n_r^q(t)$. It is clear that $\theta_r^{p,q}(t)$ linearly increases with time t.

To remove the impact of time t and modulation data (ϕ_p', ϕ_q'), replacing r by l and m in (8), we further compute the double phase difference, $\theta_{l,m}^{p,q}(t) = \theta_l^{p,q}(t) - \theta_m^{p,q}(t)$, as follows:

$$-\frac{d_l - d_m}{\lambda_{p-q}} = n_{l,m}^{p,q}(t) + \frac{1}{2\pi}\theta_{l,m}^{p,q}(t), \tag{9}$$

where $n_{l,m}^{p,q}(t) = n_l^{p,q}(t) - n_m^{p,q}(t)$ and $\lambda_{p-q} = c/(f_p - f_q)$ is an equivalent wave length corresponding to the difference between f_p and f_q. If $n_{l,m}^{p,q}(t)$ is somehow estimated, the distance difference $d_l - d_m$ can be computed from the phase information.

C. ERROR SOURCES
Several error sources may affect the system performance, as follows:

- ISI in OFDM signals. This may occur even under perfect time synchronization because of the constraint "sampling signals at different receivers at the same time", but it can be solved by adjusting the sampling time.
- Signal synchronization. The late analysis shows that this can be changed to ISI, and a small frequency difference leads to a small error.
- Multipath propagation and noise. The late analysis shows that a large frequency difference leads to a small error.
- Phase ambiguity. This must be fixed before computing distance difference by (9).

IV. DEALING WITH ERROR SOURCES
A. DEALING WITH ISI
In the system model, it is assumed that both receivers l and m compute their phases at the same time. In this way, however, it is not always possible for both receivers to avoid ISI, because the difference of ToA at two receivers is not necessarily the multiple of T_s. Figure 3 shows an example. Receiver l acquires samples at the times nT_s without ISI. But ISI occurs if receiver m acquires samples at the same time. To avoid the ISI, we let receiver m delay its sampling time by a small offset Δt ($0 \leq \Delta t < T_s$), and compensate for the phase variation.
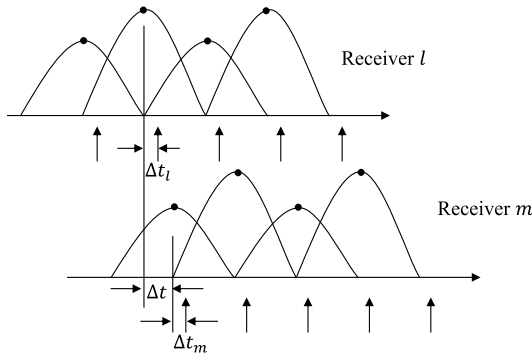
FIGURE 3. Sampling time adjustment for avoiding ISI and potential synchronization error at two receivers.

According to (8), at the time $t + \Delta t$, the phase difference at m, $\theta_m^{p,q}(t + \Delta t)$, is

$$(f_p - f_q)(t + \Delta t) - \frac{d_m}{\lambda_{p-q}} + \frac{1}{2\pi}(\phi_p' - \phi_q')$$
$$= n_m^{p,q}(t + \Delta t) + \frac{1}{2\pi}\theta_m^{p,q}(t + \Delta t). \quad (10)$$

Then, the double phase difference, $\theta_{l,m}^{p,q}(t, t + \Delta t) = \theta_l^{p,q}(t) - \theta_m^{p,q}(t + \Delta t)$ is computed from (8) and (10) as

$$-(f_p - f_q) \cdot \Delta t - \frac{d_l - d_m}{\lambda_{p-q}}$$
$$= n_{l,m}^{p,q}(t, t + \Delta t) + \frac{1}{2\pi}\theta_{l,m}^{p,q}(t, t + \Delta t), \quad (11)$$

where $n_{l,m}^{p,q}(t, t + \Delta t) = n_l^{p,q}(t) - n_m^{p,q}(t + \Delta t)$. This indicates that although two receivers sample phases at different timing, the distance difference can be computed from $\theta_{l,m}^{p,q}(t, t + \Delta t)$ if the time offset Δt is known.

Here, t at receiver l and $t + \Delta t$ at receiver m are determined by signal synchronization. In the ideal case, each receiver achieves perfect synchronization and independently decides its own sampling time. And the time offset Δt can be computed accordingly.

B. DEALING WITH SYNCHRONIZATION ERROR
In a real system, synchronization errors do occur in the receiving stage. Assume the synchronization error is Δt_l at receiver l and Δt_m at receiver m, as shown in Figure 3. In TDoA, the synchronization errors directly affect the time difference, which is $|\Delta t_m - \Delta t_l|$ and in the worst case, $|\Delta t_m| + |\Delta t_l|$.

Under synchronization errors, the timing for measuring the phase is $t + \Delta t_l$ at receiver l and $t + \Delta t + \Delta t_m$ at receiver m, respectively. From (10), we can see that a time offset Δt leads to an increase of $(f_p - f_q)\Delta t$ in the phase difference of two frequencies, irrelevant of the receiver. Then, for PDoA, the double phase difference can be represented as

$$-(f_p - f_q) \cdot (\Delta t + \Delta t_m - \Delta t_l) - \frac{d_l - d_m}{\lambda_{p-q}}$$
$$= \hat{n}_{l,m}^{p,q} + \frac{1}{2\pi}\hat{\theta}_{l,m}^{p,q}, \quad (12)$$

where $\hat{\theta}_{l,m}^{p,q}$ is computed as

$$\hat{\theta}_{l,m}^{p,q} = \theta_l^{p,q}(t + \Delta t_l) - \theta_m^{p,q}(t + \Delta t + \Delta t_m)$$
$$\approx \left(\theta_l^{p,q}(t) + 2\pi(f_p - f_q) \cdot \Delta t_l\right)$$
$$- \left(\theta_m^{p,q}(t + \Delta t) + 2\pi(f_p - f_q) \cdot \Delta t_m\right)$$
$$= \theta_{l,m}^{p,q}(t, t + \Delta t) - 2\pi(f_p - f_q) \cdot (\Delta t_m - \Delta t_l), \quad (13)$$

where $\approx$ indicates that $\theta_l^{p,q}(t + \Delta t_l)$ is not exactly equal to $\theta_l^{p,q}(t) + 2\pi(f_p - f_q) \cdot \Delta t_l$ under ISI, but the error is small considering that Δt_l is small. The same applies to $\theta_m^{p,q}(t + \Delta t + \Delta t_m)$. Under this approximation, in (12), both sides have $-(f_p - f_q) \cdot (\Delta t_m - \Delta t_l)$. Removing this item, (12) will have a similar form as (11). In this way, the synchronization error will be removed, but ISI remains a problem.

C. DEALING WITH MULTIPATH/NOISE BY AVERAGING
In (11), if p is changed from 1 to $N - 1$, and q is fixed at 0, $N - 1$ equations are obtained, as follows.

$$d_l - d_m = -c \cdot \Delta t$$
$$- \lambda_{p-q}(n_{l,m}^{p,q}(t, t + \Delta t) + \frac{1}{2\pi}\theta_{l,m}^{p,q}(t, t + \Delta t)). \quad (14)$$

Here $n_{l,m}^{p,q}(t, t + \Delta t), p = 1, 2, \cdots, N - 1, q = 0$ are unknowns, and the approximate solution can be computed by substituting the distance estimated from CSI into (14). This is usually called float solution because the estimated $n_{l,m}^{p,q}$ is a float number. The accurate solution where $n_{l,m}^{p,q}$ is fixed as an integer will be discussed late.

These $N - 1$ equations lead to $N - 1$ distance differences with different error properties. With the same channel noise, $n_{l,m}^{p,q}(t, t + \Delta t) + \frac{1}{2\pi}\theta_{l,m}^{p,q}(t, t + \Delta t)$ in (14) have almost the same variance. Then, the error in $d_l - d_m$ decreases with λ_{p-q}. This means a larger frequency difference will lead to a smaller error in the distance difference.

To suppress the impact of multipath and noise, we'd like to smooth phase difference by computing their average from multiple frequency pairs. Notice that when frequency pairs have the same difference, i.e., λ_{p-q} is the same, $n_{l,m}^{p,q}$ is the same, and $\theta_{l,m}^{p,q}$ should be the same although affected by noise and multipath propagation. Then, frequency pairs are divided into I groups so that in the i-th group, each pair has the same frequency difference, $D_i \cdot \Delta f$, where D_i is the difference between subcarrier indices. The phase differences of frequency pairs in the i-th group form a set $S_{l,m}^i = \{\theta_{l,m}^{D_i+n,n}, n = 0, 1, \cdots, N - 1 - D_i\}$, and their average is computed as

$$\overline{\theta}_{l,m}^i = \frac{1}{|S_{l,m}^i|} \sum_{n=0}^{N-1-D_i} \theta_{l,m}^{D_i+n,n}, \quad (15)$$

and the average of distance difference computed from the i-th group of frequency pairs is

$$\rho_{l,m}^i = -c \cdot \Delta t - \lambda_{D_i} \cdot (n_{l,m}^i + \frac{1}{2\pi}\overline{\theta}_{l,m}^i), \quad (16)$$

where $n_{l,m}^i$ represents the common integer ambiguity.

In the presence of noise and multipath propagation, $\theta_{l,m}^{D_i+n,n}$ of each frequency pair may differ slightly. This causes a problem when computing the average of phase difference. $\theta_{l,m}^{D_i+n,n}$ is in the range $[0, 2\pi)$ which is centered at π. A value near 2π actually is close to 0 in terms of the 2π period, although the arithmetic difference is nearly 2π. To avoid this problem, $S_{l,m}^i$ is mapped to a new set $\hat{S}_{l,m}^i$, in the range $[\overline{\theta}_{l,m}^i - \pi, \overline{\theta}_{l,m}^i + \pi)$. Specifically, if a value in $S_{l,m}^i$ is less than $\overline{\theta}_{l,m}^i - \pi$, it is added by 2π; otherwise, if it is greater than $\overline{\theta}_{l,m}^i + \pi$, it is subtracted by 2π. Then, the average of phase difference $\overline{\theta}_{l,m}^i$ is computed again over $\hat{S}_{l,m}^i$.

D. SOLVING 2π AMBIGUITY IN PHASE

Solving the 2π ambiguity in phase requires a rough estimation of $d_l - d_m$ as $\hat{d}_l - \hat{d}_m$. Although this can be computed by using RSSI or CSI, it has a relatively large error. Instead, we use TDoA [22] to get a more accurate estimation of $\hat{d}_l - \hat{d}_m$. Then, together with average phase difference $\overline{\theta}_{l,m}^i$, $n_{l,m}^i$ is estimated from $\hat{d}_l - \hat{d}_m$ as a float solution $\hat{n}_{l,m}^i$ according to (16).

With I groups of frequency pairs, we have I float solutions. From integer tuples $(n_{l,m}^1, n_{l,m}^2, \cdots, n_{l,m}^I)$ where $n_{l,m}^i \in [\hat{n}_{l,m}^i - \sigma_i, \hat{n}_{l,m}^i + \sigma_i]$ (σ_i specifies the search range of $n_{l,m}^i$), we need to find the optimal integer values (fixed solution) that best satisfy (16).

A metric is needed to evaluate the suitability of each candidate tuple $(n_{l,m}^1, n_{l,m}^2, \cdots, n_{l,m}^I)$. From each group i, we can get an estimation of distance difference $\rho_{l,m}^i = d_l - d_m$ by (16), which should be the same for all groups. Then, a simple method is to check the consistency of all distance differences. Specifically, we compute the average value $(\overline{\rho}_{l,m})$ of distance differences, and use the residual between each $\rho_{l,m}^i$ and $\overline{\rho}_{l,m}$ as the suitability metric, as follows:

$$res(n_{l,m}^1, n_{l,m}^2, \cdots, n_{l,m}^I) = \sum_{i=1}^{I} |\rho_{l,m}^i - \overline{\rho}_{l,m}|^2,$$

$$\overline{\rho}_{l,m} = \frac{1}{I} \sum_{i=1}^{I} \rho_{l,m}^i. \tag{17}$$

The integer tuple that leads to the least residual in (17) is regarded as the optimal solution. To reduce the false probability, a ratio between the second least residual and the least residual is computed. A large ratio indicates a high likelihood of the optimal solution, and usually only when the ratio is above a pre-determined threshold (e.g., 10), will the fixing process be regarded as successful [23], and a fusion, $g(\rho_{l,m}^1, \cdots, \rho_{l,m}^I)$, is regarded as the final result of distance difference. Currently, this fusion is simple average $(\overline{\rho}_{l,m})$, and more advanced fusion will be studied in the future.

The whole algorithm for computing distance difference from phase information is summarized in Algorithm 1. The computation cost of finding the optimal integer tuple (line 7) is $O((2\sigma_i)^I)$, which grows exponentially with I. Using TDoA

Algorithm 1 Compute Distance Difference by Phase Info

1: **procedure** Compute-distance-difference(θ_l^k, θ_m^k)
2:     Compute double phase difference $\theta_{l,m}^{p,q}$
3:     Divide phases into groups $S_{l,m}^i$, and convert to $\hat{S}_{l,m}^i$
4:     Compute $\overline{\theta}_{l,m}^i$ from each group $\hat{S}_{l,m}^i$
5:     Get an estimation of distance difference by TDoA
6:     Compute a float estimation of 2π ambiguity by (16)
7:     Find integer values of 2π ambiguity by (17)
8:     Compute $\overline{\rho}_{l,m}$ as distance difference
9: **end procedure**

---

instead of RSSI to estimate the distance difference enables to use a small σ_i, which helps to reduce the computation cost.

V. SIMULATION EVALUATION

In the simulation, it is assumed that a pedestrian transmits an OFDM signal with a bandwidth of 20MHz. Accordingly, the sampling interval of an OFDM signal is $T_s = 50$ ns. The duration of each OFDM symbol is 4 μs, corresponding to 80 samples, with 64 data samples and 16 samples as cyclic prefix. For simplicity, we use a training OFDM symbol for symbol synchronization and the phase information measurement. The OFDM signal passes a multipath channel with additive white Gaussian noise. At the anchors, the signal is processed at 1GHz clock, to ensure a high time resolution. The V2X frequency band, 700MHz in Japan, is used. The pulse shaping signal adopts raised cosine with a rolloff of 0.5. $\sigma_i = 1$ is used in finding the 2π ambiguity.

A. RESULT IN THE SIMPLE SCENARIO

First we consider a simple scenario composed of one transmitter and two receivers (anchors) in Figure 1. It is assumed that the 2π ambiguity, $n_{l,m}^{p,q}$, is known and that perfect synchronization is achieved.

1) SUPPRESSING ISI

Here, we investigate the effect of adjusting sampling time on suppressing ISI. To simplify the analysis, it is assumed that there is only LoS path, without multipath signals and noise at both receivers. The propagation delay to receiver l is fixed to 100 ns, and that to receiver m is adjusted from 50 ns to 100 ns.

Figure 4 and Figure 5 show the error variation of distance difference, without/with adjusting sampling time, respectively. In both figures, 5 combination of p and q are investigated, and their difference is set to 5, 10, 15, 20, 25, respectively. In Figure 4 without adjusting sampling time, at fixed p and q, the error in distance difference varies like a sine wave when the delay to receiver m increases. This error is caused by ISI at receiver m, and the error pattern depends on the pulse shaping function $f(t)$ in (2). In the left part of Figure 4, the error is positive, which means $d_l - d_m$ is greater than its true value. As d_l is fixed in this evaluation, it infers
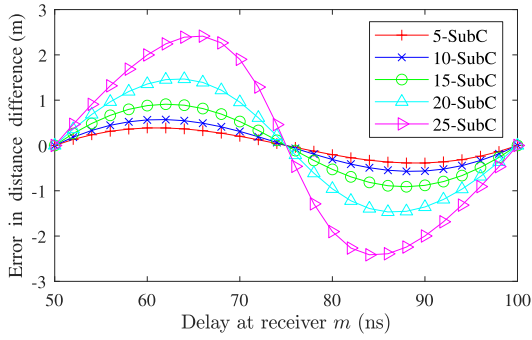
FIGURE 4. Error in distance difference with respect to the delay to receiver *m* (before adjusting sampling time).
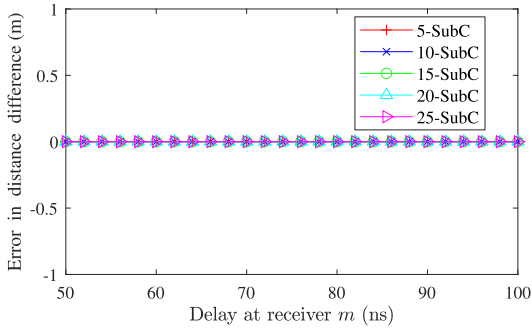

FIGURE 5. Error in distance difference with respect to the delay to receiver *m* (after adjusting sampling time).

FIGURE 6. Suppression of multipath signals by using two frequencies in estimating distance difference.
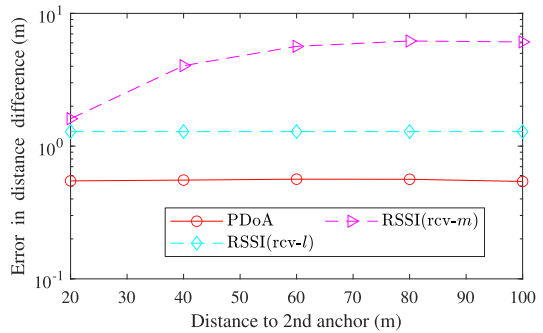
FIGURE 7. Error in distance or distance difference with respect to the distance to the receiver *m*.

that d_m is less than its true value, which can be explained as follows: In the left part, the ISI at receiver m adds to its phase. Then, as the distance to receiver m increases, the phase decrease in (7) is less than expected. In the right part, the ISI at receiver m decreases its phase and leads to the opposite result. As for the impact of p and q, the general trend is that a larger difference between p and q leads to a larger error in the distance difference.

In comparison, after adjusting the sampling time at receiver m, the error in the distance difference is almost 0, as shown in Figure 5. This confirms that adjusting the sampling time helps to avoid ISI.

2) SUPPRESSING MULTIPATH SIGNAL

Next, the impact of frequency difference on suppressing multipath signal is investigated. The delays of the direct wave from the transmitter to receivers l and m are set to 50 ns and 100 ns, respectively. For simplicity, here, we only consider one reflected wave to receiver m. Its amplitude is set to 0.3162 (in power, -10 dB) of the direct wave, and its extra delay with respect to the direct wave is set to 2, 10, 20, 50, 100 ns, respectively. There is no reflected wave to receiver l, and no noise at both receivers.

With $q = 1$ fixed and p increased from 2 to 63, Figure 6 shows the error variation in the distance difference. Generally, a large p tends to lead to a small error. Then, to effectively suppress multipath signals, it is preferred to use a large frequency difference to estimate distance difference.
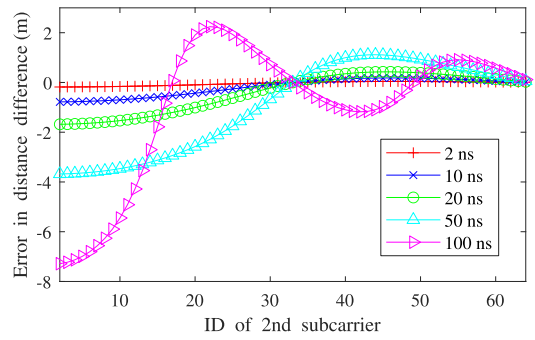
3) INSUSCEPTIBLE TO DISTANCE CHANGE/NOISE

Here, the impact of noise is investigated. The distance to receiver l is fixed to 15 m, and the distance to receiver m is increased from 20 to 100 m. Besides the direct wave, there is a reflected wave to both l and m, with a random extra delay in the range (0, 50) ns, and a random amplitude in (0, 0.3162) of that of the direct wave. At each receiver, there is additive white Gaussian noise, whose power is fixed.

The result of distance error by the RSSI and that of distance difference error by PDoA are shown in Figure 7. It is clear that the error in distance (RSSI(rcv-m)) increases with the distance when RSSI is used. This is because noise power is fixed while the signal strength decreases. In comparison, the error in distance difference by PDoA almost remains unchanged. This is because PDoA exploits phase information (which is less susceptible to noise) instead of signal amplitude, and computes average over multiple frequency pairs to further resist noise.

B. RESULT IN MULTIPATH-RICH ENVIRONMENT

Next, we will evaluate the performance of PDoA in a multipath-rich environment. The area we choose is Ginza, Tokyo, with many high buildings. The 3D building map (Figure 8) is input into the 3D ray-tracing tool, RapLab,[1] which computes all possible propagation paths. To control the computation cost, the maximum number of reflections/diffractions is set to 1. Although RapLab supports
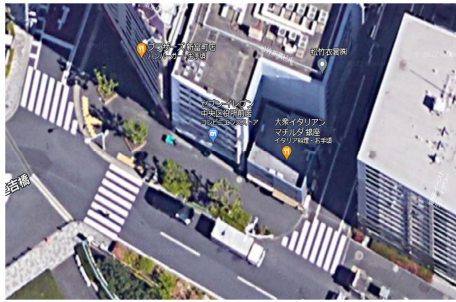
[1]https://network2.kke.co.jp/wireless-products/raplab/

FIGURE 8. 3D map used in ray-tracing simulation (Ginza, Tokyo).
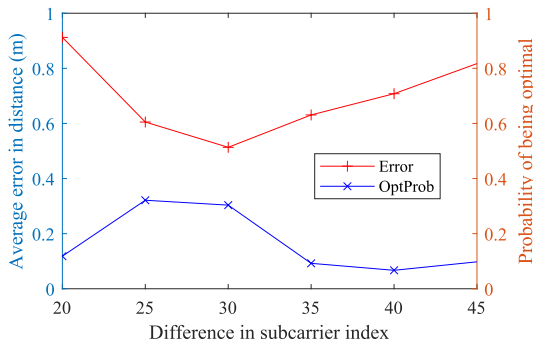
FIGURE 9. Average of absolute distance difference error per group, and the probability of being optimal.

FIGURE 10. Cumulative distribution function of error in distance difference in the multipath-rich urban canyon environment (Pedestrian-anchor distance ≤ 40 m).

fine time resolution, in the processing, the time resolution is set to 1 ns, i.e., when the difference of arrival time of two waves is less than 1 ns, their signals will overlap together, and be merged as one. Both the transmission power and noise level are fixed. Then, the received power is decided by the pedestrian-anchor distance. Besides multipath propagation, synchronization is also performed using the training symbol in the preamble of the received signal, with potential synchronization errors.

In a real system not all subcarriers are usable. Here, we use the subcarriers specified in IEEE 802.11a, in which 52 out of 64 subcarriers are used for data and pilot transmission.

At first, frequency pairs are dividing into $I = 6$ groups, with $D_i = 20, 25, 30, 35, 40, 45$, respectively. We investigate the average error of distance difference estimated from each group. The results are shown in Figure 9. It is clear that with the increase of D_i, the average error first decreases and after reaching the minimum, increases again. It should be noted that for a specific instance, the group leading to the optimal result may change, and the probability of being optimal is large when $D_i = 25, 30$.

Because computation cost grows exponentially with I while $I \geq 2$ is desired for fixing the ambiguity, in the following, we select $I = 3$, and $D_i = 25, 30, 35$. As a comparison method, the estimation of distance difference by TDoA is computed. To see the lower bound of the proposed PDoA method, the method that always selects the distance difference with the minimal error from I groups is also simulated, which is denoted as PDoA-Opt.

In the evaluation, multiple vehicles on the roads are used as anchors, and the anchor with the minimal distance to the
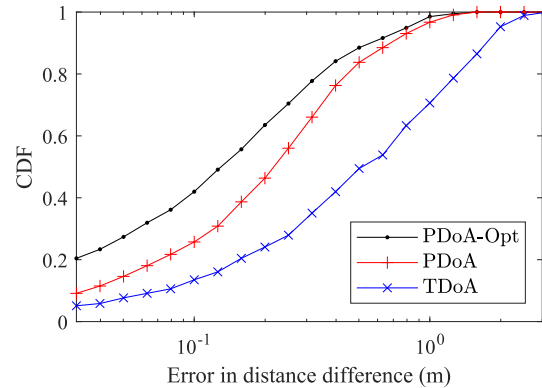
pedestrian is regarded as a reference. Other anchors form pairs with the reference anchor to compute the distance difference.

First, we only select anchors with a pedestrian-anchor distance less than 40 m. Figure 10 shows the cumulative distribution function (CDF) of errors in distance difference. Obviously, PDoA reduces large errors compared with TDoA. An investigation shows that these large errors in TDoA are caused by synchronization error, which are converted to smaller ISI errors in PDoA. The root mean squared error (RMSE) is 0.370, 0.454 and 1.106 m in PDoA-Opt, PDoA, and TDoA, respectively. There is a small gap between PDoA and PDoA-Opt, because the latter always selects the value with the minimal error, which, however, is difficult in practical systems. In PDoA, the probability that the error is less than 1.0 m is 0.967, which is very promising.

If we allow the pedestrian-anchor distance increase up to 70 m to use more anchors, the RMSE will change to 0.626, 0.779, and 1.446 in PDoA-Opt, PDoA, and TDoA, respectively. In PDoA, the probability that the error is less than 1.0 m is 0.869, which is still very high.

In summary, the proposed PDoA method helps to resist ISI of OFDM signals and synchronization error, and suppress the impact of multipath error and noise by combining multiple subcarriers. In addition, using TDoA helps to reduce the search range (computation cost) in fixing the phase ambiguity, and the result of the PDoA method is close to the optimum.

VI. CONCLUSION

Different from previous methods that use signal strength to estimate distance, this paper has tried to use the phase information, which is more resistant to multipath propagation and noise. In the model, a pedestrian transmits a V2X OFDM signal, and the phase information of multiple frequencies is measured efficiently and simultaneously at several anchors, based on which PDoA is estimated and the distance difference is computed. The analysis shows that (i) error factors such as OFDM modulation data and carrier frequency variations can be mitigated, (ii) ISI can be avoided by adjusting the sampling

time, (iii) PDoA is less susceptible to synchronization error compared with TDoA, (iv) Using multiple frequency pairs helps to suppress multipath and fix phase ambiguity. The result in the multipath-rich environment is promising.

As a first step, for simplicity, we did not consider pedestrian speed. In the evaluation, it is assumed that a pedestrian stays at a fixed position without movement. In the future, we will evaluate the impact of the Doppler effect due to pedestrian speed, further investigate how to better fuse the results computed from multiple frequency differences, and study the positioning method.

REFERENCES

[1] Cabinet Office in Japan. (2020). *White Paper on Traffic Safety in Japan.* [Online]. Available: https://www8.cao.go.jp/koutu/taisaku/r03kou_haku/english/pdf/wp2021-2.pdf

[2] S. Tang, K. Saito, and S. Obana, "Transmission control for reliable pedestrian-to-vehicle communication by using context of pedestrians," in *Proc. IEEE Int. Conf. Veh. Electron. Saf. (ICVES)*, Nov. 2015, pp. 41–47.

[3] J. Kotte, C. Schmeichel, A. Zlocki, H. Gathmann, and L. Eckstein, "Concept of an enhanced V2X pedestrian collision avoidance system with a cost function–based pedestrian model," *Traffic Injury Prevention*, vol. 18, pp. S37–S43, May 2017.

[4] J. Paziewski, "Recent advances and perspectives for positioning and applications with smartphone GNSS observations," *Meas. Sci. Technol.*, vol. 31, no. 9, Jun. 2020, Art. no. 091001, doi: 10.1088/1361-6501/ab8a7d.

[5] S. Tang and S. Obana, "Improving performance of pedestrian positioning by using vehicular communication signals," *IET Intell. Transp. Syst.*, vol. 12, no. 5, pp. 366–374, Jun. 2018.

[6] W. Komamiya, S. Tang, and S. Obana, "Precise angle estimation by jointly using spatial/temporal change of channel state information and its application in pedestrian positioning," *IEEE Access*, vol. 9, pp. 59420–59431, 2021.

[7] G. Naik, B. Choudhury, and J.-M. Park, "IEEE 802.11bd & 5G NR V2X: Evolution of radio access technologies for V2X communications," *IEEE Access*, vol. 7, pp. 70169–70184, 2019.

[8] S.-W. Ko, H. Chae, K. Han, S. Lee, D.-W. Seo, and K. Huang, "V2X-based vehicular positioning: Opportunities, challenges, and future directions," *IEEE Wireless Commun.*, vol. 28, no. 2, pp. 144–151, Apr. 2021.

[9] Q. Liu, P. Liang, J. Xia, T. Wang, M. Song, X. Xu, J. Zhang, Y. Fan, and L. Liu, "A highly accurate positioning solution for C-V2X systems," *Sensors*, vol. 21, no. 4, p. 1175, Feb. 2021. [Online]. Available: https://www.mdpi.com/1424-8220/21/4/1175

[10] F. Mogyorósi, P. Revisnyei, A. Pašić, Z. Papp, I. Törös, P. Varga, and A. Pašić, "Positioning in 5G and 6G networks—A survey," *Sensors*, vol. 22, no. 13, p. 4757, Jun. 2022. [Online]. Available: https://www.mdpi.com/1424-8220/22/13/4757

[11] S. Sen, J. Lee, K.-H. Kim, and P. Congdon, "Avoiding multipath to revive inbuilding WiFi localization," in *Proc. 11th Annu. Int. Conf. Mobile Syst., Appl., Services (MobiSys)*, Jun. 2013, pp. 249–262.

[12] Z. Yang, Z. Zhou, and Y. Liu, "From RSSI to CSI: Indoor localization via channel response," *ACM Comput. Surveys*, vol. 46, no. 2, pp. 1–32, Dec. 2013, doi: 10.1145/2543581.2543592.

[13] A. Makki, A. Siddig, M. Saad, J. R. Cavallaro, and C. J. Bleakley, "Indoor localization using 802.11 time differences of arrival," *IEEE Trans. Instrum. Meas.*, vol. 65, no. 3, pp. 614–623, Mar. 2016.

[14] D. Feng, C. Wang, C. He, Y. Zhuang, and X.-G. Xia, "Kalman-filter-based integration of IMU and UWB for high-accuracy indoor positioning and navigation," *IEEE Internet Things J.*, vol. 7, no. 4, pp. 3133–3146, Apr. 2020.

[15] A. Povalac and J. Sebesta, "Phase difference of arrival distance estimation for RFID tags in frequency domain," in *Proc. IEEE Int. Conf. RFID-Technol. Appl.*, Sep. 2011, pp. 188–193.

[16] G. von Zengen, Y. Schröder, S. Rottmann, F. Büsching, and L. C. Wolf, "No-cost distance estimation using standard WSN radios," in *Proc. 35th Annu. IEEE Int. Conf. Comput. Commun. (IEEE INFOCOM)*, Apr. 2016, pp. 1–9.

[17] H. Chen, T. Ballal, N. Saeed, M.-S. Alouini, and T. Y. Al-Naffouri, "A joint TDOA-PDOA localization approach using particle swarm optimization," *IEEE Wireless Commun. Lett.*, vol. 9, no. 8, pp. 1240–1244, Aug. 2020.

[18] S. Tang and S. Obana, "Exploiting phase difference of arrival of V2X signals for pedestrian positioning," in *Proc. IEEE VTC-Fall*, Sep. 2022, pp. 1–6.

[19] L. Banin, O. Bar-Shalom, N. Dvorecki, and Y. Amizur, "High-accuracy indoor geolocation using collaborative time of arrival," IEEE, Piscataway, NJ, USA, Tech. Rep. IEEE 802.11-17/1397R0, 2017.

[20] M. Bullmann, T. Fetzer, F. Ebner, M. Ebner, F. Deinzer, and M. Grzegorzek, "Comparison of 2.4 GHz WiFi FTM- and RSSI-based indoor positioning methods in realistic scenarios," *Sensors*, vol. 20, no. 16, p. 4515, Aug. 2020. [Online]. Available: https://www.mdpi.com/1424-8220/20/16/4515

[21] J. Choi, "Enhanced Wi-Fi RTT ranging: A sensor-aided learning approach," *IEEE Trans. Veh. Technol.*, vol. 71, no. 4, pp. 4428–4437, Apr. 2022.

[22] F. Gustafsson and F. Gunnarsson, "Positioning using time-difference of arrival measurements," in *Proc. IEEE Int. Conf. Acoust., Speech, Signal Process. (ICASSP)*, vol. 6, Apr. 2003, p. 553.

[23] P. J. G. Teunissen and S. Verhagen, "The GNSS ambiguity ratio-test revisited: A better way of using it," *Surv. Rev.*, vol. 41, no. 312, pp. 138–151, Apr. 2009.

SUHUA TANG (Senior Member, IEEE) received the B.S. degree in electronic engineering and the Ph.D. degree in information and communication engineering from the University of Science and Technology of China, in 1998 and 2003, respectively. From October 2003 to March 2014, he was with Adaptive Communications Research Laboratories, ATR, Japan. Since April 2014, he has been with the Graduate School of Informatics and Engineering, The University of Electro-Communications, Japan. His research interests include green communications, ad hoc and sensor networks, inter-vehicle communications, and high precision positioning. He is a member of IEICE and IPSJ.

SADAO OBANA received the B.E., M.E., and Ph.D. degrees from Keio University, Tokyo, Japan, in 1976, 1978, and 1993 respectively. After joining KDDI (former KDD), in 1978, he was engaged in research and development in the field of packet exchange systems, network architecture, open systems interconnection (OSI) protocols, database, distributed processing, network management, and intelligent transport systems (ITS). In 2004, he joined the Advanced Telecommunication Research Institute International (ATR), where he was the Director of Adaptive Communications Research Laboratories. From 2011 to 2018, he was a Professor with the Graduate School of Informatics and Engineering, The University of Electro-Communications, Japan, where is currently the Executive Director. He received an Award of Minister of Education, Culture, Sports, Science and Technology, in 2001. He is a member of The Institute of Electronics, Information and Communication Engineers (IEICE) and a fellow of Information Processing Society of Japan (IPSJ).

• • •